COUPLING BETWEEN THE LOWER ATMOSPHERE AND THERMOSPHERE AS REVEALED IN GOCE AND SWARM ACCELEROMETER MEASUREMENTS

Jeffrey M. Forbes [(1)], Xiaoli Zhang [(1)], Jesse Zhang [(1)], Eelco Doornbos [(2)], Sean L. Bruinsma [(3)]

[(1)] Department of Aerospace Engineering Sciences, University of Colorado, Boulder, CO 80309, USA, Email: forbes@colorado.edu

[(2)] Delft Institute of Earth Observation and Space Systems, Delft University of Technology, Kluyverweg 1, 2629 HS Delft, The Netherlands, Email: E.N.Doornbos@tudelft.nl

[(3)] Department of Terrestrial and Planetary Geodesy, CNES, 18, avenue E. Belin, 31401 Toulouse Cedex 9, France, Email: sean.bruinsma@cnes.fr

ABSTRACT

A major discovery of the last decade is that tropospherically-generated solar and lunar tides extend well into the ionosphere-thermosphere (IT) system, and drive ionosphere and neutral density variability pertinent to the operation of communications and navigation systems, and orbital and re-entry predictions. This paper describes how density and wind measurements from accelerometers on CHAMP, GRACE and GOCE are used to elucidate this vertical coupling that occurs in the atmosphere. A few new results are provided for GOCE, and some insights into how Swarm will contribute are described as well.

1. INTRODUCTION

Within the last decade, a new realization has arrived on the scene of ionosphere-thermosphere (IT) science: ***terrestrial weather significantly influences space weather.*** The aspect of space weather of relevance here, of course, consists of the variability of neutral densities and winds that define the drag on satellites and determine their future locations, and the ionosphere variability that impacts operational communications and navigation systems. As illustrated in Figure 1, the primary mechanism through which energy and momentum are transferred from the lower atmosphere to the upper atmosphere and ionosphere is through the generation and propagation of waves. Periodic absorption of solar radiation in local time (LT) and longitude by tropospheric H_2O and stratospheric O_3 excites a spectrum of thermal tides with periods of 24h (diurnal), 12h (semidiurnal), and so on. Surface topography and unstable shear flows excite planetary waves (PW) and gravity waves (GW). PW are either quasi-stationary (i.e., they do not propagate zonally or do so at very slow speeds) or are oscillations at periods near 2, 5, 6.5, 10, and 16 days, and occasionally at other periods. They are often related to natural quasi-resonances in the atmosphere, but can sometimes arise through, or be amplified by, instabilities, which are enabled by mean wind shears forced by solar inputs and momentum deposited by GWs. Absorption of solar radiation at the surface and the subsequent release of latent heat of evaporation in convective clouds radiates additional thermal tides, GWs, and other classes of waves. The moon's gravity also generates lunar tides that propagate vertically. Vertically-propagating waves grow exponentially with height into the more rarified atmosphere, ultimately achieving large amplitudes. Some parts of the wave spectrum achieve convective instability, spawning additional waves or turbulence. Other parts of the wave spectrum are dissipated by molecular diffusion, and some fraction of the wave population penetrates all the way to the base of the exosphere (ca. 500-600 km). Along the way, nonlinear interactions between different wave types occur, modifying the interacting waves and giving rise to secondary waves. Finally, the IT wind perturbations carried by the waves can redistribute ionospheric plasma, either through the electric fields generated via the dynamo mechanism, or directly by moving plasma along magnetic field lines.

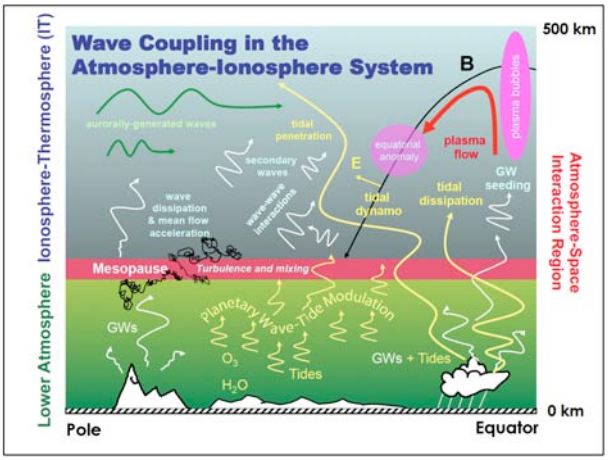

Figure 1. The primary mechanism through which energy and momentum are transferred from the lower atmosphere to the upper atmosphere and ionosphere is through the generation and propagation of waves. In the ionosphere wind perturbations associated with the waves can redistribute ionospheric plasma, either through the electric fields generated via the dynamo mechanism, or directly by moving plasma along magnetic field lines.

Proc. 'ESA Living Planet Symposium 2013', Edinburgh, UK
9–13 September 2013 (ESA SP-722, December 2013)

In this paper we briefly summarize how density and wind measurements on satellite missions like CHAMP, GRACE, GOCE and Swarm can reveal the signatures of waves that originate in the lower atmosphere and propagate well into the thermosphere. Since Swarm data are not yet available, we restrict ourselves to a few illustrations using CHAMP, GOCE and GRACE data, and then outline what Swarm is expected to contribute in the future. Due to time and space restrictions, we restrict our discussion to solar thermal and lunar gravitational tides, while recognizing that these missions also have much to offer in terms of studying the planetary and gravity waves mentioned previously.

Before proceeding further, some notations used throughout this paper are defined. We adopt the mathematical form $A_{n,s}\cos(n\Omega t+s\lambda-\varphi_{n,s})$ to represent a tidal oscillation in any atmospheric variable, where $A_{n,s}$ is the amplitude, n = 1, 2, 3 refers to diurnal, semidiurnal and terdiurnal (periods of 24h, 12h, 8h, respectively), $\Omega=2\pi/24h$, s is the zonal wavenumber, λ is longitude and $\varphi_{n,s}$ is the phase (time of maximum at λ = 0). A tide that migrates with the westward motion of the Sun to a ground-based observer corresponds to s = n and appears the same at all longitudes. Longitudinal variability projects onto a range of longitudinal wavenumbers, s, at each frequency; these waves are referred to as non-migrating tides. In this context we utilize the notation DWs or DEs to denote a westward or eastward-propagating diurnal tide, respectively, with zonal wavenumber = s. For semidiurnal oscillations 'S' replaces 'D'. The zonally-symmetric oscillations are denoted D0, S0. Stationary planetary waves with zonal wavenumber m are denoted 'SPWm'.

2. BRIEF REVIEW OF SOLAR TIDE GENERATION IN THE TROPOSPHERE

Although non-migrating tides receive non-negligible excitation from solar radiation absorption in the troposphere, the largest contribution originates from the latent heating that occurs in connection with tropical convection [1,2]. A very simplified presentation in the following gets across the main ideas. If we imagine the sun passing over the surface of the Earth, evaporating surface moisture which convects upward, and then releases the latent heat of evaporation, we can see how latent heating is released on a diurnal cycle in the atmosphere. Moreover, if we recognize that this occurs much more effectively over land than ocean, we can see how the distributions of oceans vs. land control the longitude variability of this diurnal cycle. Now, consider that the major zonal Fourier component of land-sea difference is m = 4 at low latitudes, and that the solar heating driving the convective cycle has a local time harmonic that varies as $\cos(\Omega t + \lambda)$ to a ground-based observer (omitting the phase, φ, hereafter); in other words, the solar radiation imparted to the surface "migrates" westward with a speed of $\Omega = 2\pi/24h$. The wave-4 topography modulates this solar heating like so: $\cos(4\lambda) \times \cos(\Omega t + \lambda)$ to produce the "sum" and "difference" waves:

$$\cos(\Omega t + 5\lambda) + \cos(\Omega t - 3\lambda)$$

which are recognized as DW5 and DE3 according to our notation. Similarly, there is a semidiurnal harmonic of the solar radiation, $\cos(2\Omega t + 2\lambda)$ (with the same zonal phase speed), that interacts with the wave-4 component of land-sea difference to produce the sum and difference waves SW6 and SE2. Additional waves are generated by interactions with other land-sea difference zonal wavenumbers. DW5 is dissipated before it reaches the ionosphere-thermosphere (IT), but DE3, SE2 and SW6 are observed there. The following discussion mainly concentrates on DE3 and SE2.

3. SOLAR TIDES FROM CHAMP, GRACE, GOCE and Swarm

CHAMP, GRACE, GOCE, Swarm are all either Sun-synchronous or quasi-Sun-synchronous. A tide represented by $\cos(n\Omega t + s\lambda)$ can be represented in terms of local time as $\cos(n\Omega t_{LT} + (s-n)\lambda)$. Thus from quasi-Sun-synchronous orbit ($t_{LT} \approx$ constant), a tide with frequency n day^{-1}, and zonal wavenumber s generated by wave-m topography appears as a wave-m longitude variation.

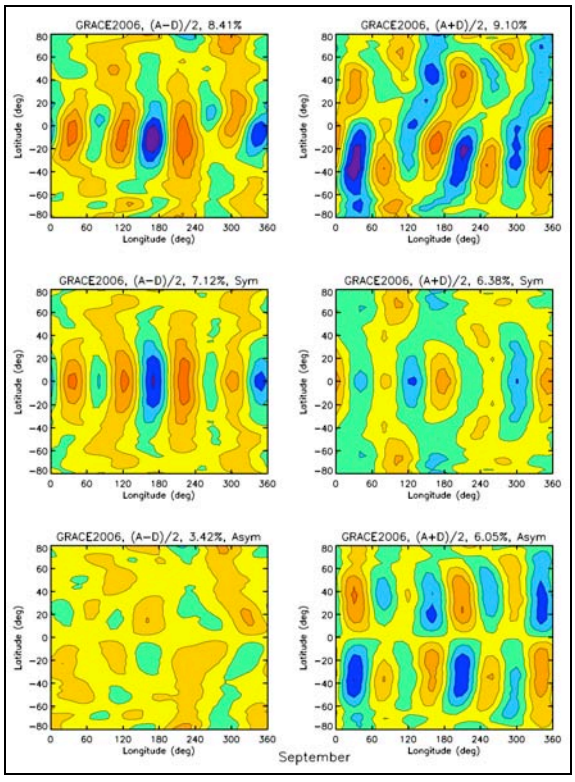

Figure 2. Top: Ascending-descending node differences (left) and sums (right) for GRACE density residuals averaged over a 10-day period in September, 2006, with wave-1 in longitude removed. Middle panels illustrate the symmetric part about the equator, and lower panels show the antisymmetric part.

"Snapshots" of sums and differences (A-D)/2 and (A+D)/2 of ascending (A) and descending (D) orbital data, ~12h apart, can be used to separate diurnal and semidiurnal tides. For instance, (A-D)/2 contains all diurnal, terdiurnal (i.e., odd-frequency), etc., waves, and (A+D)/2 contains all stationary planetary, semidiurnal, (even-frequency) waves. However, ambiguity remains as to the mixture of waves, since more than one wave can give rise to the same longitudinal wave structure, or (s-n). In this case other constraints can sometimes be applied to narrow the choices. An example is provided in Figure 2, which illustrates these sums and differences for GRACE density residuals averaged over a 10-day period in September, 2006, with wave-1 in longitude removed. In addition, these structures are decomposed into symmetric and antisymmetric parts. Given the wave-4 [(s-n) = 4] nature of these, the symmetric structure for (A-D)/2 is interpreted as DE3, whose symmetric part is an equatorially-centered Kelvin wave, and the anti-symmetric part for (A+D)/2 is very similar to theoretically-produced simulations for SE2. The symmetric part of (A+D)/2 is likely SW4. These are the types of analyses and interpretations that will be done with GOCE density and wind data, noting that the wind information will provide additional constraints on the interpretation.

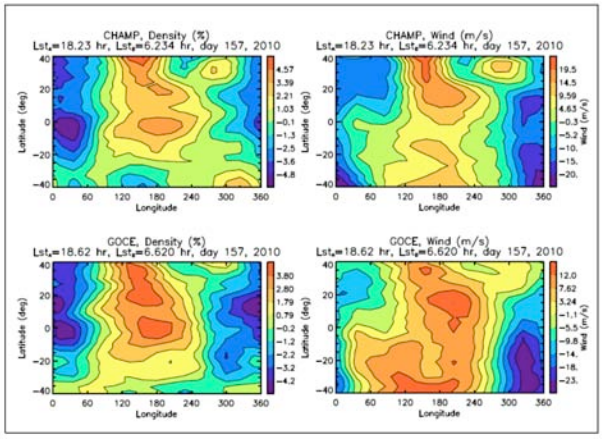

Figure 3. Comparison between CHAMP (top) and GOCE (bottom) density residuals (left) and zonal winds (right), averaged over 10 days centered on the co-planar event on day 157 of 2010.

Figure 3 compares CHAMP (~320 km altitude) and GOCE (~270 km altitude) density and zonal (cross-track) wind residuals, averaged over 10 days centered on the co-planar event on day 157 of 2010. The agreement in structures between the two satellites serves as a mutual validation between them. However, the dominance of a wave-1 structure is surprising given previous similar analyses with other satellites [3]. This may be related to the relatively low altitudes compared to CHAMP and GRACE, to the low solar activity, or to the effects of displaced geographic and geomagnetic coordinates under the above conditions. The reasons are under investigation.

As illustrated in Figure 4, The diurnal tidal spectrum evolves with height, the larger-scale waves penetrating to 400 km, while the shorter-scale waves are absorbed at intervening altitudes, giving up their energy and momentum to the mean atmosphere. There are also nonlinear interactions between the different wave components that give rise to secondary waves. Interactions with the longitudinally-varying ionosphere give rise to additional wave components. GOCE thus provides a key "middle thermosphere" perspective, between lower thermosphere measurements up to 110 km by TIMED, and upper thermosphere measurements by CHAMP, GRACE and Swarm.

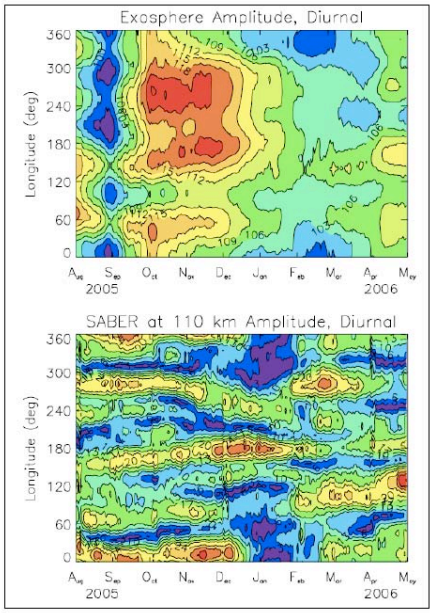

Figure 4. Equatorial diurnal tidal temperature amplitudes as a function of longitude and month from August 2005 to May 2006. (top) Exosphere temperatures, ranging from 97K (maroon) to 121K (red). (bottom) SABER temperatures at 110 km, ranging from 3K (maroon) to 27K (orange). The diurnal tidal spectrum evolves with height, the larger-scale waves penetrating to 400 km, while the shorter-scale waves are absorbed at intervening altitudes, giving up their energy and momentum to the mean atmosphere.

Some initial insight into the longitude structures observed by GOCE are provided in Figure 5, where sum and difference components are compared between GRACE during 2009 and GOCE during 2009 and 2010 for the density field. First of all, we see that the GOCE structures are very similar between 2009 and 2010, which confirms that we are looking at a quasi-fixed feature for the month of November. This agreement also serves as a kind of internal validation for the GOCE data. We also note the similarity in (A+D)/2 structures between GOCE during 2009 and the structures indicated by GRACE at much higher altitudes. Dynamical coupling between the two altitude regions by the same wave components is suggested. On the other hand, this similarity does not exist for (A-D)/2, suggesting that this part of the wave spectrum is evolving with height.

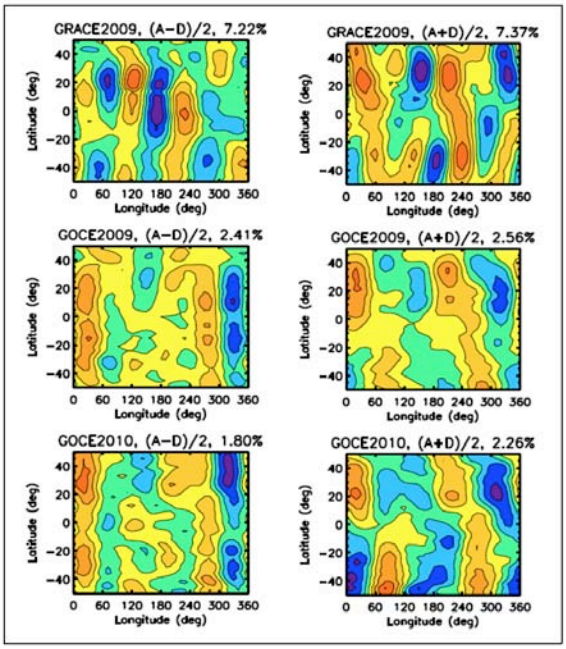

Figure 5. Comparison between ascending-descending node differences (left) and sums (right) for density residuals averaged over 10-day intervals during November, with wave-1 removed. Top: GRACE during 2009. Middle: GOCE during 2009. Bottom: GOCE during 2010.

A different way of observing solar tides in satellite data is provided in Figure 6. The bottom panel shows the latitude-time evolution of DE3 in the temperature field between May 2009 and February 2010. For satellites like TIMED, which samples 24 hours of local time in 60 days (assuming both ascending and descending node sampling), mean tides within 60-day moving windows can be performed. For CHAMP and Swarm-A/B, the window is 130 days; Swarm-C, 160 days.

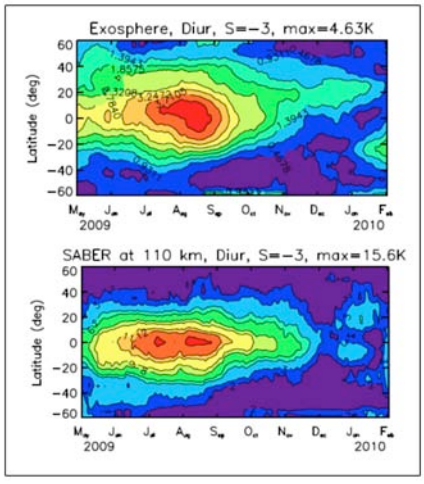

Figure 6. Bottom: 60-day running mean DE3 temperature amplitudes at 110 km derived from TIMED/SABER temperature measurements during May 2009 - February 2010. Top: 72-day running-mean DE3 exosphere temperature amplitudes (ca. 300-400 km) derived from CHAMP and GRACE density measurements during the same period.

From CHAMP and GRACE density measurements, exospheric temperatures can be derived using empirical models, and used to derive tides within 72-day windows containing 24-hour local time coverage [4]. In Figure 6 we illustrate the DE3 temperature amplitude in the upper thermosphere over the same time period using this approach. The similarity between the TIMED and CHAMP-GRACE results is consistent with the vertical propagation of DE3 from the lower thermosphere to the upper thermosphere, and moreover provides evidence that density variability at orbital altitudes is driven in part by deep convection in the tropical troposphere.

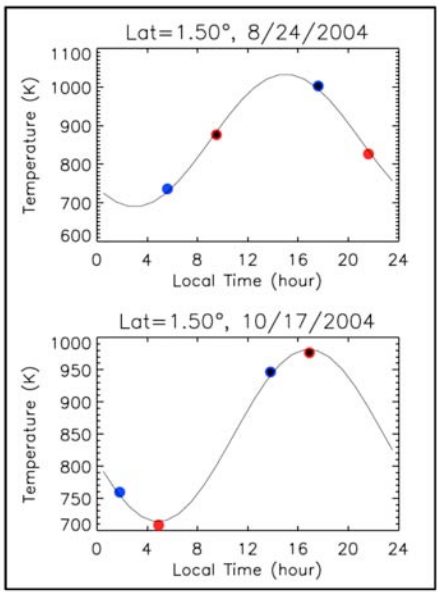

Figure 7. Samples of fits to CHAMP (red) and GRACE (blue) zonal-mean equatorial temperatures; the color dots with smaller black dot inside are the ascending nodes. The top panel shows the fit when the orbital planes are close to orthogonal, whereas the bottom panel corresponds to the case where the local times of CHAMP and GRACE are close to 3 hours separation.

The above methodology cannot be used with GOCE since the orbital plane of GOCE does not precess in local time. However, there is another method that can be used with GOCE, e.g., in combination with CHAMP, GRACE or Swarm [5]. It is based on the same fundamental principles employed in the previous method, that is, that height-independent exosphere temperatures can be derived from multiple satellites using empirical models, and then combined together to extract tidal signals. In [5] we have found that by combining CHAMP and GRACE data when orbital planes are > 3 hours LT apart, diurnal variations in exosphere temperature can been obtained on a daily basis. Examples of two fits from this study are shown in Figure 7. Figure 8 illustrates application of this method to a period of time during 2009 when the above requirement is met. We see that application of this method provides insight into the variability of DE3 over

much shorter time scales than has been achieved before. A shortcoming of the method is that it can only be applied to the diurnal tide unless a few more data points are available.

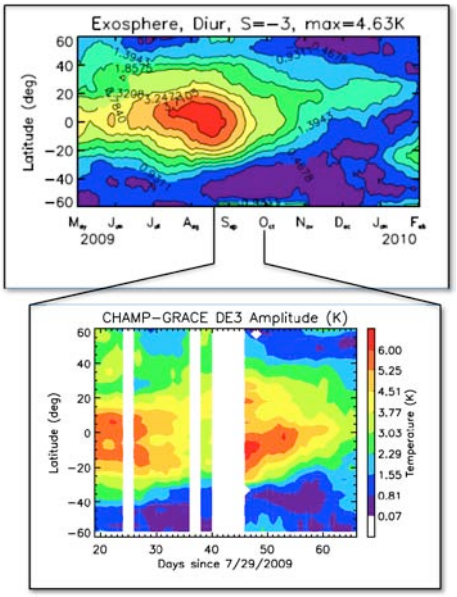

Figure 8. Top: The same 72-day running-mean depiction of DE3 temperature amplitudes shown in the top panel of Figure 6. Bottom inset: Daily DE3 amplitudes derived from CHAMP and GRACE exosphere temperatures using the type of fitting illustrated in Figure 7.

Another example using this method is provided in Figure 9. Here we illustrate the latitude vs. time evolution of the diurnal migrating tide (DW1), which is largely forced by the absorption of solar EUV radiation in the thermosphere. This example depicts the response of DW1 to the quasi-27-day variation in solar flux due to rotation of the Sun, as indicated by the 10.7-cm solar radio flux in this figure.

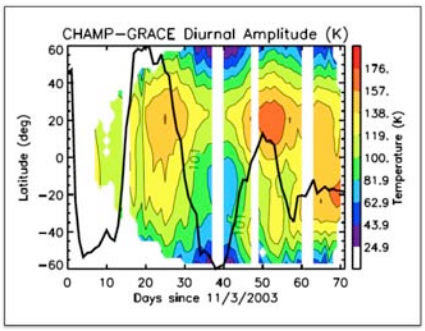

Figure 9. Daily DW1 amplitudes derived from CHAMP and GRACE exosphere temperatures using the type of fitting illustrated in Figure 7. Note the correlation with solar-rotation variability of F10.7 illustrated by the black line.

Looking to the future, the minimum 3-h LT separation between Swarm A/B and Swarm C is exceeded after 18 months, and GRACE and GOCE could provide additional data points early in the Swarm mission. In addition, similar analyses can be performed on electric fields measured by Swarm, thus providing new insights into the connection between solar tides and the electrodynamic effects that they produce through the dynamo mechanism.

4. GOCE AND THE LUNAR TIDE

The lunar tide has been studied for many decades, and there are several reasons why its study remains relevant today. First, since the gravitational forcing is reasonably well-known, observations of the lunar tide can serve as a good test of the veracity of theoretical models of wave propagation, dissipation, wave-mean flow interactions, etc. Furthermore, it is now known that the lunar tide can be considerably amplified during sudden stratospheric warmings (SSWs), and produce significant low-latitude ionospheric effects by driving electric fields through the dynamo mechanism – "ionospheric space weather" [6,7]. The lunar tide also produces significant density variations at orbital altitudes – "thermosphere space weather" – that remain unmodeled, and yet are to a significant degree predictable. GOCE provides a "middle thermosphere" perspective on the lunar tide, in terms of both density and wind variations.

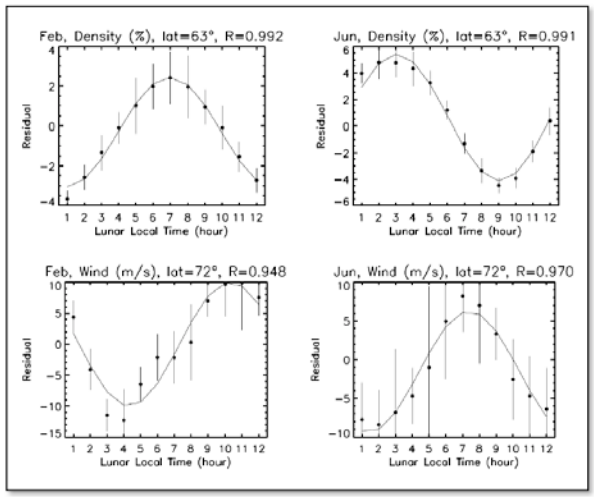

Figure 10. Examples of semidiurnal fits to GOCE density and wind residuals (from 15-day running mean) in lunar time.

Figures 10 and 11 provide an initial preliminary look at the lunar tide in the middle atmosphere as viewed by the GOCE accelerometers. The results in Figure 11 obtained by binning longitude-averaged residuals from 15-day running mean into lunar time bins covering Nov 2009 – May 2012, and extracting the amplitude of the semidiurnal lunar tide. Only low magnetic activity days are included. These are viewed as vector-average tides over this time interval. Figure 10 provides a few examples of the actual fits in lunar time, and the standard deviations of the points that are fit.

For the density field, during November-January there is a low-latitude maximum in the S. Hemisphere, and during February-March this is replaced by maxima in

each hemisphere at middle to high latitudes. The lunar tide in density is relatively small during March-May and September-November. During May-June there is a broad maximum extending from high latitudes in one hemisphere to high latitudes in the other, whereas during July-August amplitudes get smaller and weak maxima occur in each hemisphere. Amplitudes of these maxima are of order 2-5%. Similar features are seen in the GSWM simulations [e.g., 8] except that only a single low-latitude maximum is seen in the S. Hemisphere during November to March, and during May to September there is one distinct maximum in each hemisphere located roughly between 30°N and 60°N and between 10°S and 50°S. The GSWM also indicates density maxima of order 2-5%.

The wind field exhibits similar structures to the densities, except that during May-September the broad latitudinal structure seen in the densities is replaced by two maxima situated between 60°S-90°S and 60°N to 90°N. Lunar tidal wind amplitudes are generally of order 7-15 ms^{-1}. The GSWM wind results are similar to the GSWM densities, except that the wind maxima shift 10-20° poleward in each hemisphere; amplitudes of the maxima are of order 10 ms^{-1}.

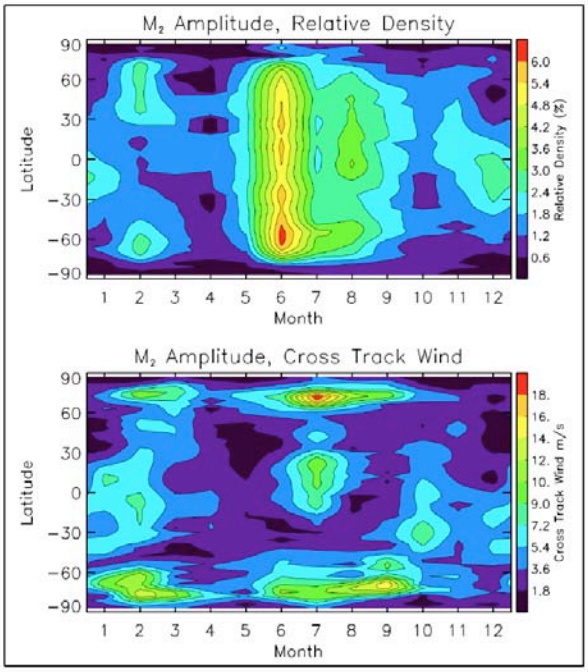

Figure 11. Lunar semidiurnal density amplitudes (top) and zonal wind amplitudes (bottom) obtained from GOCE as a function of latitude and month using the binning method illustrated in Figure 11. These represent vector averages over the November 2009 - May 2012 time period.

In conclusion, the lunar tidal results from GOCE reveal some similarities and differences in comparison to existing model results, in particular the larger latitudinal extent of the lunar tide seen in the GOCE data. The reasons for these differences are not yet clear, and the analysis would probably benefit from a year or more additional data to smooth out the rough edges. In addition, the June data require further examination in terms of coverage and data quality. These efforts are ongoing.

5. CONCLUSIONS

Our conclusions are as follows:

(1) Waves propagating upward from the lower atmosphere under go "differential dissipation" in the thermosphere, and thus their relative importance varies with height; other factors also affect the wave spectrum.

(2) At ~270 km, GOCE provides insight into vertical evolution of tidal spectrum from ~110 km (SABER) to ~400-500 km (CHAMP, GRACE, Swarm).

(3) High-precision density and wind measurements enable investigation of smaller-amplitude waves, such as lunar tides and gravity waves emanating from the polar regions and from the lower atmosphere.

(4) The combination of densities and winds provides additional constraints on decomposition of tidal components.

(5) With 2 local time measurements, GOCE will be used with CHAMP, GRACE, and Swarm in terms of obtaining sufficient local time coverage to unambiguously identify tidal components.

(6) GOCE data are already challenging theory and models.

6. REFERENCES

1. Zhang, X., J. M. Forbes, and M. E. Hagan, Longitudinal variation of tides in the MLT region: 1. Tides driven by tropospheric net radiative heating (2010a), *J. Geophys. Res., 115*, A06316, doi:10.1029/2009JA014897.

2. Zhang, X., J. M. Forbes, and M. E. Hagan, Longitudinal variation of tides in the MLT region: 2. Relative effects of solar radiative and latent heating (2010b), *J. Geophys. Res., 115*, A06317, doi:10.1029/2009JA014898.

3. Forbes, J. M., X. Zhang, and S. Bruinsma (2012), Middle and upper thermosphere density structures due to nonmigrating tides, *J. Geophys. Res., 117*, A11306, doi:10.1029/2012JA018087.

4. Forbes, J. M., S. L. Bruinsma, X. Zhang, and J. Oberheide (2009), Surface-exosphere coupling due to thermal tides, *Geophys. Res. Lett., 36*, L15812, doi:10.1029/2009GL038748.

5. Forbes, J. M., X. Zhang, S. Bruinsma, and J. Oberheide (2011), Sun–synchronous thermal tides in exosphere temperature from CHAMP and GRACE accelerometer measurements, *J. Geophys. Res., 116*, A11309, doi:10.1029/2011JA016855.

6. Fejer, B. G., M. E. Olson, J. L. Chau, C. Stolle, H. Lühr, L. P. Goncharenko, K. Yumoto, and T. Nagatsuma, Lunar dependent equatorial ionospheric electrodynamic effects during sudden stratospheric warmings (2010), *J. Geophys. Res., 115*, A00G03,doi:10.1029/2010JA015273.

7. Fejer, B. G., B. D. Tracy, M. E. Olson, and J. L. Chau, Enhanced lunar semidiurnal equatorial vertical plasma drifts during sudden stratospheric warmings (2011), *Geophys. Res. Lett., 38*, L21104, doi:10.1029/2011GL049788.

8. Forbes, J.M., X. Zhang, S. L. Bruinsma, and J. Oberheide (2013), Lunar semidiurnal tide in the thermosphere under solar minimum conditions, *J. Geophys. Res., 118,* doi:10.1029/2012JA017962.